Acta Cryst. (1970). A26, 414

Principles of Electron Structure Research at Atomic Resolution Using Conventional Electron Microscopes for the Measurement of Amplitudes and Phases

BY W. HOPPE

Abteilung für Röntgenstrukturforschung am Max-Planck-Institut für Eiweiss- und Lederforschung, München, und Physikalisch-Chemisches Institut der Technischen Hochschule München, Abteilung für Strukturforschung, München, Germany.

(*Received* 18 *August* 1969)

An electron microscope equipped with conventional electron optics can be used as a 'diffractometer' for structure research on individual aperiodic objects. The resolution limit of the electron microscope is not the resolution limit of the 'diffractometer' and electron structure research with atomic resolution is possible. The advantage is that a diffractometer of this type can measure amplitudes and phases. The theory is developed in the language of the crystallographer, mainly using the concept of modifying functions. It is shown that, as in crystallography, redundancies in structures can be used in the analysis.

Introduction

Structure analysis at atomic resolution has been confined until now to problems where the scattering of a single atom could be amplified by the scattering of many other geometrically equivalent atoms, for example in crystal structure analysis and analysis of gases and liquids. There is no doubt that a structure analysis of individual aperiodic objects at atomic resolution would be of extreme interest. The only chance to do this is to use electrons or other strongly scattered particles. One could argue that the object will be destroyed before a sufficient number of scattered particles has been collected. The excellent results at 'atomic resolution' with the field ion microscope have shown that this is not true for all objects. On the other hand, the structure work itself could analyse how atomic configurations of various kinds, and gases in vacuum react with electrons* for example.

An especially interesting diffraction instrument for electrons is the electron microscope. It has the enormous advantage that it yields not only the amplitudes but also the phases of the scattered electron waves. The difficulty is that the limited resolving power of existing electron microscopes does not allow micrograms to be made at atomic resolution. There are other difficulties as well, but the resolution difficulty is a fundamental one. The simplest way to cope with this limit would be to make electron lenses with smaller aberrations. However, contrary to light optics, this problem turns out to be extremely complicated. Sophisticated devices have been proposed (*e.g.* Scherzer & Typke, 1967/68), but the difficulties in building and aligning them will be substantial. Several years ago, it was shown (Hoppe, 1961, 1963) that the resolution limit of an electron microscopic objective of conventional design (*i.e.* having a magnetic field with rotational symmetry) is not a real limit. It was demonstated that there are new ways to achieve atomic resolution with an electron microscope of low resolving power. In the meantime it has become evident that there are several ways of utilizing the resolution-extending principle put forward in the first publications. It will be shown later that the possible solutions can be divided into two classes: zone correction methods and image reconstruction methods. The special solution, proposed in 1961, belongs to the first class. Combinations of both schemes are possible and useful.

It often happens in science that work along new lines leads to surprising and unexpected implications in other directions. Image reconstruction methods are characterized by many manipulations in reciprocal space. The image itself is then synthesized in an analogue or digital computer. It will be shown in this paper that the reconstruction process can be generalized in such a way that the real physical structure, not influenced by the properties of the microscope, can be extracted. Thus, the electron microscope becomes a tool for structure analysis comparable to a diffractometer, the only difference being that it measures amplitudes and phases.

In this paper, a theory covering the aspects of both classes of method will be given. As the aim of this use of electron microscopes is structure research, the theory will be written in the language of the crystallographer. This has an additional advantage. It is well-known that restrictions in the shape of the atomic configuration make it possible to solve structures in crystallography without knowledge of phases. In the electron structure analysis with the electron microscope, the phase problem does not exist, but for other reasons, the information might be incomplete. The knowledge of basic structural features may also make

* Radiation damage need not be irreparable. It depends on whether reverse reactions to the initial structures can take place.

it possible to cope with restrictions in information in this case. A part of this paper is devoted to these redundancy problems.

The optical problem

A comparison of the optical properties of a light microscope and of an electron microscope reveals remarkable differences. In the light microscope, the resolution limit is given by the diffraction limit. There is no difficulty in correcting for spherical aberration, the only aberration which is important in microscopy.*

In electron microscopy, there is no difficulty with the diffraction limit, but one has to contend with spherical aberration. Glaser has defined a 'best resolution', using an aperture where the spherical aberration is approximately equal to diffraction aberration. The principle can best be explained if one introduces the pupil function of a lens:

$$P=\exp i\gamma(\theta)\,. \tag{1}$$

Reduced to a magnification 1 it follows that for image points near the optical axis (Scherzer, 1949):

$$\gamma(\theta)=\frac{2\pi}{\lambda}(\tfrac{1}{2}Z_0\theta^2-\tfrac{1}{4}C_{\ddot{o}}\theta^4) \tag{2}$$

The wave aberration γ describes the phase shift of the diffracted rays caused by the non-spherical wave surface. γ depends on the spherical aberration constant $C_{\ddot{o}}$, on the distance z_0 of the (plane) object from the focus, and, of course, on the scattering angle θ for a given wavelength λ. Fig. 1 shows the real and imaginary parts of P calculated for the Gaussian image plane ($z_0=0$) for two objectives with $C_{\ddot{o}}=4$ and $C_{\ddot{o}}=1$ *mm*. The first example corresponds to the conventional Elmiskop I objective, the second example to something like an objective of conventional design with the lowest spherical aberration which could be incorporated without undue difficulties into a conventional 100kV microscope. The lowest spherical aberration constant ($C_{\ddot{o}}=0{\cdot}5$ mm) has been achieved by Ruska & Riecke in their one field condensor objective (Ruska, 1965). For an ideal lens ($C_{\ddot{o}}=0$) it would follow that $P=1$ in the Gaussian image plane. This means that the real part of this function could be characterized in Fig. 1 by a straight line parallel to the θ axis while the imaginary part would be zero for all scattering angles in the Gaussian plane ($z_0=0$). By the use of such a lens, correct imaging would be possible for amplitude objects. Zernike (1935) has shown that an ideal lens for phase objects corresponds to $P=\pm i$ for $\theta\neq 0$ (*i.e.* real part is zero and the imaginary part is ± 1 for all $\theta\neq 0$). It is easy to see in Fig. 1 that for a small range of θ (*i.e.* small aperture) P corresponds quite well to an ideal lens for amplitude objects. Glaser (1952) has shown that the imaging properties of an ideal lens will be retained in approximation if the real part of P remains positive in the non screened-off θ range. This limit is marked in the real parts of Fig. 1 by arrows. A similar argument for the same sign of the imaginary part leads to a resolution limit for phase objects (again marked by arrows in Fig. 1). The

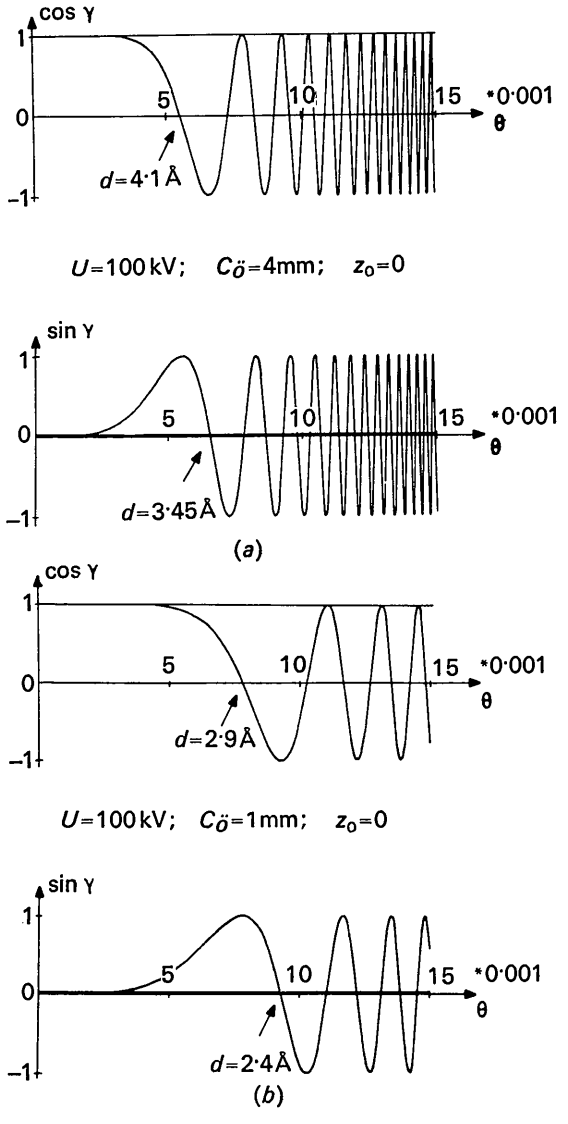

Fig. 1. Pupil functions of a conventional electron microscopical objective as functions of the scattering angle θ. $U=100$ kV, $C_{\ddot{o}}=4$ mm (*a*), $C_{\ddot{o}}=1$ mm (*b*), Gaussian plane. The arrows show the limiting scattering angle corresponding to the Glaser resolution limit for amplitude objects (real part, cos γ) and for phase objects (imaginary part, sin γ). The corresponding Abbe resolutions d ($=0{\cdot}6\ \lambda/\sin\theta$) are given for comparison. Note that the resolution limit for phase objects is higher. On the other hand the phase contrast for small scattering angles is small. The real and imaginary parts of the pupil function in this regions can be regarded as modifying functions in the sense of Waser & Schomaker (1953).

* Chromatic aberration can also be corrected, but this is of minor importance because chromatic aberration could be minimized by the use of monochromatic radiation. Axial astigmatism, unknown in light optics, is more an imperfection than an aberration. Correction is possible in the instrument.

next important step was made by Scherzer (1949). He showed that the θ ranges of the same sign can be considerably enlarged if one includes in equation (2) a small defocusing term ($z_0 \neq 0$). Fig. 2 shows the pupil function P for the same examples as Fig. 1. The Glaser aperture can, therefore, be replaced by the larger Scherzer aperture and the sharpest image will then occur at the Scherzer focus. The next idea for the enlargement of the resolution limit was put forward in 1961 (Hoppe, 1961, 1963). Fig. 3 illustrates the principle, again for the two examples $C_{\ddot{o}}=4$ and $C_{\ddot{o}}=1$ mm. Employing again the defocusing parameter z_0 of equation (2), one can obtain pupil functions of the type shown in Fig. 3. These functions do not oscillate too rapidly in the ranges of θ marked by the arrows. The reason for the oscillations is the periodic nature of P for all $\gamma_n=\gamma_0+2\pi n$ (where n is an integer), $P_n=P_0$. Using the criterion of the same sign, correct imaging could for example be achieved for phase objects, if the positive regions of the imaginary parts in Fig. 3 were to be screened off by a system of annular screens. Then only the negative parts contribute to the image. But of course the transferred information will to some extent be incomplete. The question is only whether the missing parts of the Fourier transform will obscure the image. We will return to this point later.

This screening off must be done in the aperture plane of the objective (*e.g.* using zone-correction plates). It can also be carried out by other filtering processes which will be discussed in the course of this paper.

There is an alternative way of applying similar corrections. In conventional electron microscopes, the aperture of the illumination is much smaller than the aperture of the objective. Thus, the illumination is not only monochromatic but also spatially coherent. Let us now assume that there is a weakly scattering object. ϱ is the complex amplitude formed by the superposition of all scattered waves (with the exception of the primary wave) and A is the amplitude of the primary wave. (Propagation is along the optical axis.) The intensity in the image plane is then given by equation (3).

$$I=I_0^2+I_0(\varrho+\varrho^*)+\varrho\varrho^* \qquad (3)$$

The important point is that the intensity distribution in the image plane is proportional to the real part of ϱ [*i.e.* the second term in equation (3)] since the third term can be neglected if $\varrho \ll I_0$*. This linear relation between amplitude and intensity also means a close resemblance between the Fourier transform of ϱ (which is responsible for the distribution in the aperture plane) and the Fourier transform of the intensity distribution. Therefore, the necessary corrections to the pupil function can be made in two steps. The distorted intensity distribution is first registered on a photographic plate, and in the second step, the Fourier transform of this distribution is generated in a light diffractometer or by computation.

In this Fourier transform the Fourier coefficients in the regions $\left(\frac{4n-1}{2}\right)\pi<\gamma>\left(\frac{4n+1}{2}\right)\pi$ (amplitude object) will have the correct phases. The phases of the other Fourier coefficients can now be corrected by a

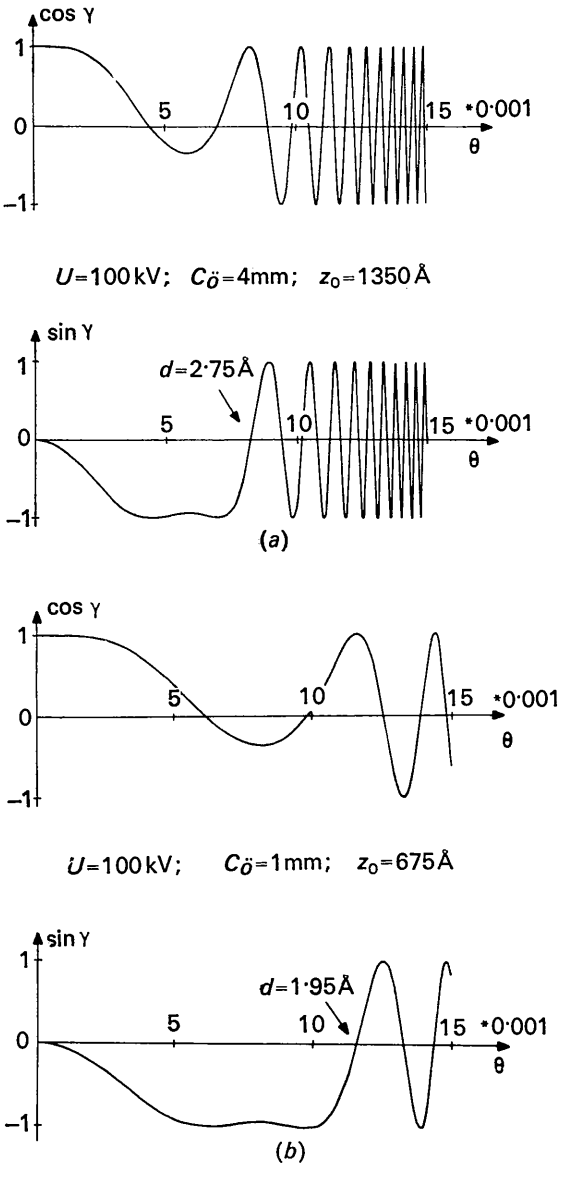

Fig. 2. Pupil functions, calculated for Scherzer's definition of resolving power by introducing a defocusing term $z_0 \neq 0$. Note that the defocusing term chosen in these examples enlarges the resolution limit for phase objects but reduces the resolution limit for amplitude objects (*cf.* Fig. 1). The sign of phase contrast is reversed.

* If one combines a bright field image with a dark field image ($I_0=0$), one can separate the second and the third term in equation (3).

phase shift of using a π phase-shifting plate in the light diffractometer* or by computation and a corrected image can be reconstructed. 'Double diffraction' procedures of that type were first used by Maréchal & Croce (1953) in light optics for the correction of defocused photographic images. As $C_{\ddot{o}}$ can be made zero in light optics, only the first term in equation (2) will be present. Hanszen (1968) and Schiske (1968) have proposed using the Maréchal process in a special version which will be discussed later.

Light optics with coherent illumination has been rapidly developed in recent years, stimulated by the extensive use of laser sources. It is interesting to see that the methods of coherent light optics for the correction of lens aberrations can be used in electron optics. But the similarity of tools does not mean similarity in problems. In light optics, spherical aberration is an unimportant parameter. With $C_{\ddot{o}}=0$, the number of nodes in the pupil function can be fixed arbitrarily for a deliberately chosen aperature simply by adjusting the defocusing parameter z_0. If $C_{\ddot{o}}\neq 0$, then the minimal number of nodes depends on the aperture. This number increase rapidly if the maximum angle of scattering is substantially enlarged. The number of nodes, however should not be excessive. It is possible to resolve the pupil function in the aperture plane. This resolution depends on the coherence of the primary wave and on the chromatic aberration. Surprisingly enough, only a factor of about 2 to 3 can be gained, compared with the resolution limits in Figs. 1 and 2, but it is this gain which allows us to use a conventional electron microscope as a tool for structure analysis at atomic resolution.

The structure problem

We shall consider the electron microscope as a diffractometer. Fig. 4 shows the principal relation in reciprocal space. x^*,y^*,z^* denote the Cartesian coordinates† in reciprocal space, corresponding to x,y,z coordinates in real space. Coherent illumination in the electron microscope means definition of a single primary beam vector $\mathbf{s}_0/\lambda$. The orientation of the primary beam vector will be along the z^* axis in reciprocal space.‡ At atomic resolution all electron microscopical objects must be considered as three-dimensional objects: in fact, they must be regarded as thick objects. A foil of only 50 Å thickness already has the dimensions of a protein molecule. This means that the three-dimensional structure (*i.e.* three-dimensional Fourier transform) should be studied. One direction of illumination and one wavelength mean that only points on the surface of the Ewald sphere in reciprocal space can be reached. The answer for the study of three-dimensional Fourier transforms, almost trivial in the case of X-ray structure analysis, is either to rotate the specimen for a fixed wavelength or to change the wavelength for a given orientation. The first method has independently been proposed with somewhat different experimental procedures by De Rosier & Klug (1968) and by Hoppe, Langer, Knesch & Poppe, (1968). The latter method will be difficult to apply to electrons, as the acceleration voltage of the electrons must be lowered to about 1V.

With high energy electrons (50—100 kV) only a small region of the theoretically accessible reciprocal space, necessary for atomic resolution, can be reached in the electron microscope. This region, defined by the opening of the aperture diaphragm, is marked schematically in Fig. 4 by the small sphere around the origin of reciprocal space.

Let us first make a general comment. The problem is to register at a given orientation and at a given resolution an intensity function with a detector (*e.g.* a photographic plate) which can be converted into the Fourier transform of the object. The intensity function is a real function expressed for example as a density in the plate. From general Fourier transform principles it follows that the object function must also be a real function, if the registration is to take place without information loss, but the Fourier transform of a complex function will result for two reasons:

1. The atoms are complex scatterers ('anomalous dispersion'). The phases vary with the type of atom.
2. The Fourier coefficients lie on a curved surface (*i.e.* on the Ewald sphere).

The Fourier coefficients of a real function obey the Friedel rule. If we denote the vector in reciprocal space by $\mathbf{r}^*$ then $F_{-\mathbf{r}^*}=F^*_{\mathbf{r}^*}$. If all atoms scatter anomalously but with the same phase shift (*e.g.* if only atoms of the same kind are present) the Friedel rule is also valid.

A curved surface in reciprocal space for a given orientation will lead to a formal invalidity of the Friedel rule even in the case of a real structure simply because there are pairs $F_{\mathbf{r}^*}$ and $F_{-\mathbf{r}^*}$ only in approximation (*cf.* Fig. 4). The deviation from centrosymmetry increases with $\mathbf{r}^*$.

We have now been confronted for the first time with a general feature of electron structure analysis using an electron microscope as a diffractometer. In general it is not possible to obtain complete information with one exposure only. Two ways exist of coping with this difficulty:

---

* Light diffractometers in electron microscopy were first used by Klug & Berger (1964) with great success for the study of structural features of objects at medium resolutions where no electron optical problems occur. The first use of light diffractometers for the study of electron optical constants under conditions of phase contrast and at the limit of resolution has been proposed by us and verified in experiments by Thon (1966) (see also page 422).

† For aperiodic objects Cartesian (cubic) coordinates are the simplest choice, unless special symmetries in the object (as in crystallography) suggest more general coordinates.

‡ Illumination inclined to the optical axis is sometimes useful. The generalization of the theory to this case is straight forward.

1. One can make several exposures under different conditions, provided that in the combination of the diagrams the complete information can be found. Several exposures will be necessary for the three-dimensional scan of the Fourier transform by rotation of the specimen.

2. A knowledge of structural features will be used to complete the information.

In order to develop the theory properly, it is useful to generalize the well-known concept of modifying functions which has been introduced into X-ray crystallography by Waser & Schomaker (1953), if the structure factor (Fourier transform) of an aperiodic object is given by:

$$F_{x^*y^*z^*} = \sum_{j=1}^{n} f_j \exp 2\pi i(x^*x_j + y^*y_j + z^*z_j) \quad (4)$$

then this Fourier transform can be converted into a Fourier transform of the same geometrical structure but with modified atoms simply by multiplication of the Fourier transform by a modifying function S:

$$F'_{r^*} = SF_{r^*} = \sum_{j=1}^{n} Sf_j \exp 2\pi i(x^*x_j + y^*y_j + z^*z_j) . \quad (5)$$

The shape of the modified atoms ϱ'_j is given by the convolution of the unmodified atom ϱ_j with the Fourier transform σ of the modifying function S:

$$\varrho'_j = \widehat{\varrho_j \sigma} . \quad (6)$$

The modifying functions in crystallography (sharpening of Patterson peaks, weighting functions in reciprocal space, transformation of real atoms into unitary, normalized, Gaussian atoms) are real and positive functions. Now all types of real or complex functions are allowed. A second generalization concerns the introduction of the individual modifying function S_j:

$$F'_{r^*} = \sum_{j=1}^{n} S_j f_j \exp 2\pi i(x^*x_j + y^*y_j + z^*z_j) . \quad (7)$$

As can be seen from equation (7) this procedure again retains the geometrical structure of the atomic configuration. But the shapes of the different atoms will be altered in different ways.* Combinations of both modifications are possible.

It is useful to specify a special class of modifying functions as 'back-modifying functions'. Their definition is given in equation (8).

$$SS^- = u \quad (8)$$

u is a real and positive function. In the ideal case u should be equal to unity, but in order to avoid that S^- becomes excessevely large for very small values of S (or for other reasons) one might be forced to use a $u<1$ for certain regions in the reciprocal space. The modification with S^- will change F'_{r^*} to F_{r^*}. If u is not equal to unity, the back-modification process leads to F''_{r^*} given in equation (9):

$$F''_{r^*} = uF_{r^*} . \quad (9)$$

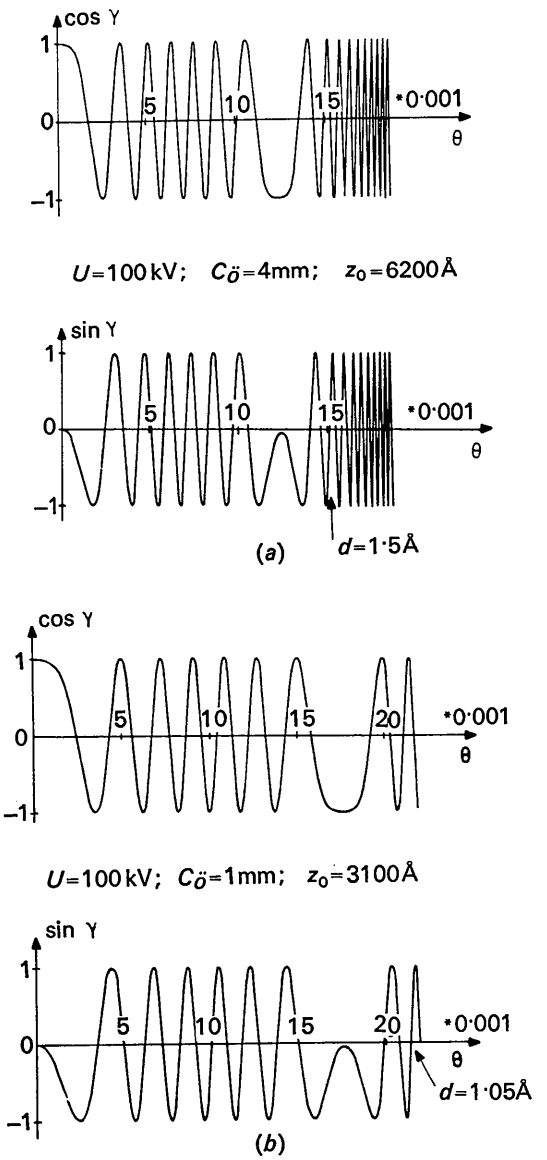

Fig. 3. Pupil functions, calculated for $z_0 \neq 0$, corresponding to the principles of zone correction plates and image reconstruction methods. The arrows separate the slowly oscillating regions of the pupil function from the rapidly oscillating regions. The destructive influence of the changing sign of amplitude contrast or phase contrast on the image point can be removed by screening off (*e.g.* for phase objects) the positive regions of the imaginary part in the figure using zone diaphragms or reversing the positive sign (phase correction zone plates or Maréchal image reconstruction). Note that the resolution limit in this special case (8 zones) will be approximately doubled compared with the Scherzer resolution limit.

* A possible use of (7) could for example be the transfer of an X-ray structure to a neutron structure. Another application, related to some extent to results in this paper, would be the presentation of general projections.

F''_{r^*} will be a good approximation of F_{r^*}, because u has been defined as a positive number between zero and unity. In this case, the back-modified atomic shape will not deviate appreciably from the real atomic shape. The modifying functions in equations (5) and (7) have been defined for the three-dimensional case. The microscope acts as a two-dimensional Fourier synthesizer; therefore, for illumination along z^* (Fig. 4), equations (5) and (7) can be replaced by equations (10) and (11):

$$F'_{x^*y^*}=S\sum_{j=1}^{n} f_j \exp 2\pi i(x^*x_j+y^*y_j)\,, \qquad (10)$$

$$F'_{x^*y^*}=\sum_{j=1}^{n} S_j \exp 2\pi i(x^*x_j+y^*y_j)\,. \qquad (11)$$

It is now easy to recognize that the phase shifting or pupil function [equation (1)] can be regarded as a modifying function. An important modification is necessary. Since atoms are phase objects an additional phase shift of $\frac{\pi}{2}$ will occur. The pupil-modifying function S_0 can, therefore, be written

$$S_0=\exp i\left(\gamma(\theta)+\frac{\pi}{2}\right). \qquad (12)$$

$\gamma(\theta)$ is given in equation (2). In the case of a thick object equation (2) must be replaced by the more general expression:

$$\gamma_j(\theta)=\gamma_0(\theta)+\frac{\pi}{\lambda} zj\theta^2\,. \qquad (13)$$

z_j is the z parameter of an atom with respect to the defocusing parameter z_0 in equation (2). Equation (13) takes into account that in a thick object the focus for every atom will be different.

$$S_j=\exp i\left(\gamma_j(\theta)+\frac{\pi}{2}\right). \qquad (14)$$

Equation (14) is then an individual modifying function which modifies F_{r^*} to F'_{r^*} in equation (7).

The interesting point is that the geometric structure will be retained in the image, even if imaging is done with aberrations. Only the shape of the atoms will be changed. But this change will make it difficult to recognize the atoms in the image. Owing to the special type of modifying functions in equations (12) and (14) the modified atoms will be spread over large regions in real space and will show a complicated internal structure. Therefore, considerable overlap of different atoms will occur. Only in the case of the Glaser or Scherzer resolution limit will the atoms have a point extension. It is also important to note that in this case the modified atoms become complex, even if the real Born approximation for the atomic scattering factors is used. Fig. 5 shows the real part and the imaginary part of a modified C atom calculated for the Glaser and Scherzer resolution limits. With coherent illumination, only the real part will be registered [equation (3)]. Note that there is a region of opposite sign around the real part of the atom, which Scherzer has already mentioned. The reason is that the real part of the modified scattering factor starts from zero (Fig. 5).* Fig. 6 now shows the real part and the imaginary part of the modified C atom, modified with the pupil function of Fig. 3. Again only the real part can be recorded on a photographic plate. The complicated extended atomic structure is immediately apparent.

Individual modifying functions mean that atoms with different z_j parameters will have different shapes. Back-modification can only take place for a deliberately chosen plane within the thick object and is not associated with lens properties. 'Focusing-through' is also well-known in light microscopy with ideal microscopic lenses. The interesting point is that this difficulty disappears if one regards a microscope as a three-dimensional diffraction instrument. Equation (13) can be rewritten as equation (15) if one introduces a z^* parameter.

$$\gamma_j=\gamma_0+2\pi z^*z_j\,,$$
$$z^*=\frac{1}{2\lambda}\theta^2\,. \qquad (15)$$

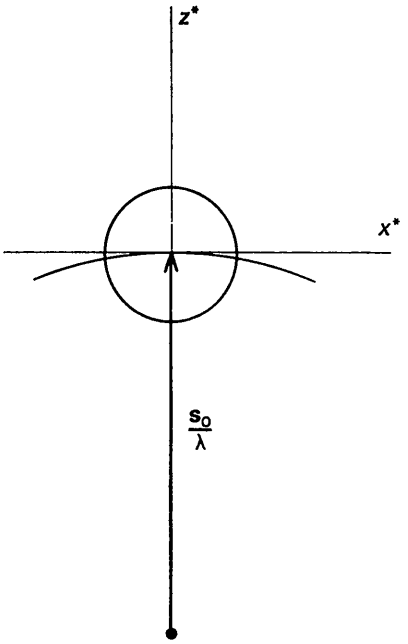

Fig. 4. The Ewald sphere for the electron microscope and definition of the coordinates x^*, y^*, z^* of reciprocal space. The optical axis and direction of the illuminating vector s_0/λ are along z^*.

* One of the modifying functions, which Waser has introduced into X-ray crystallography for other reasons, modifies the atoms in a similar way (Waser, 1953).

Introducing equation (15) into (14) and (14) into (11), one gets the three-dimensional Fourier transform

$$F'_{x^*y^*z^*} = S_0 \sum_{j=1}^{n} f_j \exp 2\pi i(x^*x_j + y^*y_j + z^*z_j) . \quad (16)$$

A simple calculation shows that z^* becomes

$$z^* = \frac{\lambda}{2}(x^{*2} + y^{*2}) \quad (17)$$

In equation (16) the modification will be done with the non-individual modifying function S_0 from equation (12). Inspection of equation (16) and (17) shows that the Fourier transform values $F_{x^*y^*z^*}$ occupy the surface of a sphere with the radius $1/\lambda$ This is not surprising since only points on the surface of the Ewald sphere can be reached in a diffraction experiment. The most important point is that the modifying function becomes non-individual. Approximations for the back-modification process are, therefore, unnecessary. Moreover, the focusing plane can to some extent be deliberately chosen. Another implication concerns the calculation of three-dimensional structures by rotating the object. The reciprocal planes have to be replaced by segments of the Ewald

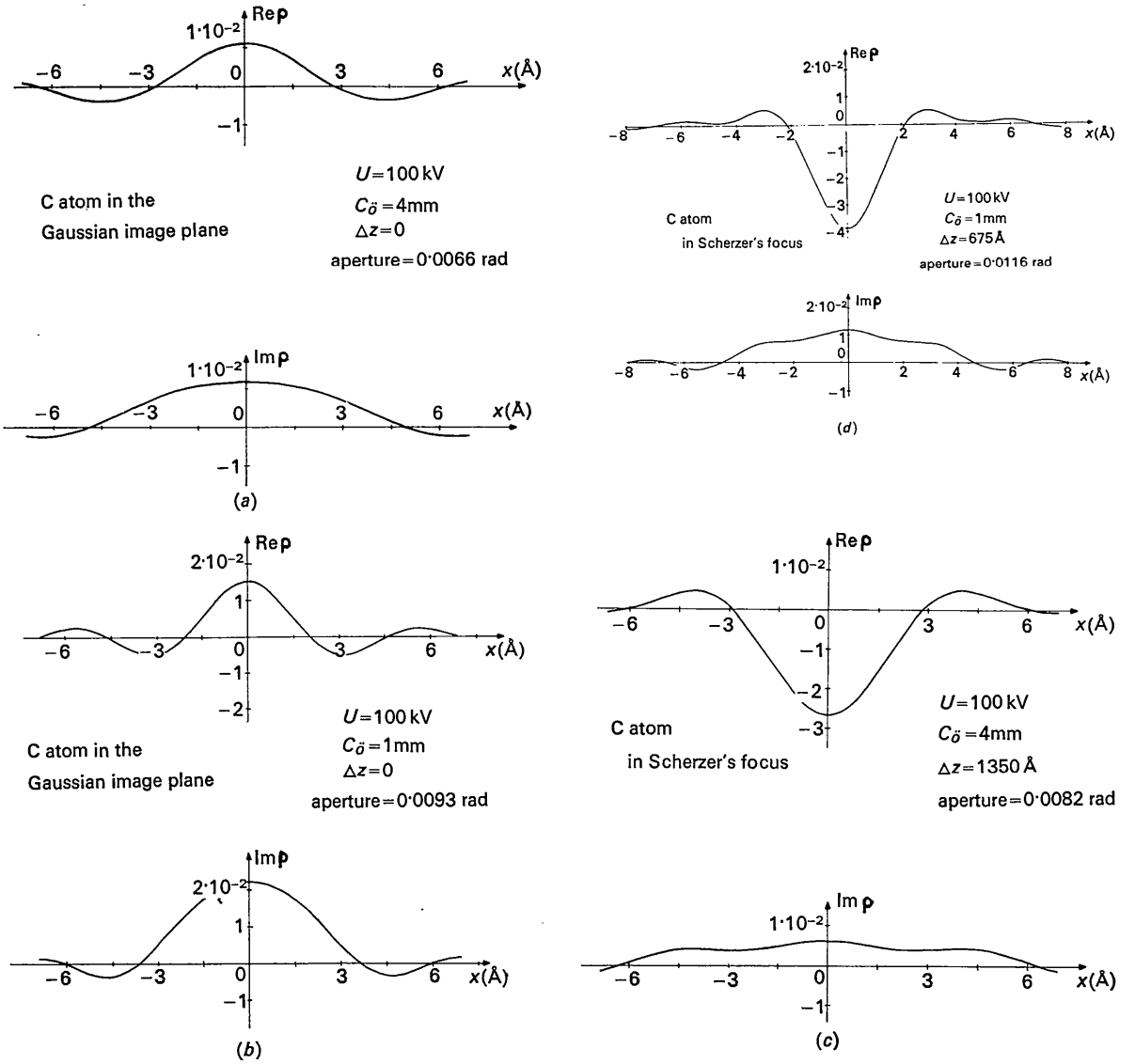

Fig. 5. Real and imaginary parts Re ϱ and Im ϱ of the complex image amplitude ϱ of a single C atom calculated for Glaser and Scherzer resolutions and the pupil functions in Figs. 1 and 2. In the bright-field image, only the real part can be seen. The substantial amelioration of the image for the Scherzer focus [Fig. 5(*c*) and (*d*)] compared with the image in the Gaussian plane [Fig. 5(*a*) and (*b*)], Glaser resolution] is immediately apparent. Note the reversed sign of Re ϱ at Scherzer resolution and compare the corresponding negative sign of the imaginary part of the pupil function in Fig. 2. The Scherzer resolutions are approximately 3 Å ($C_{\vec{\sigma}}$=4 mm) and 2 Å ($C_{\vec{\sigma}}$=1 mm). According to equation (3) in a bright field the image amplitude of the atom will be 1–2 Re ϱ.

sphere. It is of fundamental importance that an infinite depth of focus is not necessary for three-dimensional reconstruction. As we have seen an electron microscope can be used as a diffractometer which, under the assumption of coherent illumination, delivers the modified structure factor $F'_{x^*y^*}$ on the surface of the Ewald sphere [equations (16) and (17)]. The non-individual modification function is given in equation (12) [*cf.* equations (1) and (2)]. In the image plane the complex image amplitude ϱ' given by

$$\varrho'_{xy} \sim \iint F'_{x^*y^*} \exp\left[-2\pi i(x^*x+y^*y)\right]\mathrm{d}x^*\mathrm{d}y^* \quad (18)$$

will be formed. In the detector (*e.g.* a photographic plate) only the intensity [equation (3)] can be registered. In the case of weakly scattering particles the third term of (3) can be neglected. Back-modification processes are defined as processes which convert the modified structure factors F' as well as possible into the unmodified structure factor F [equation (4)].

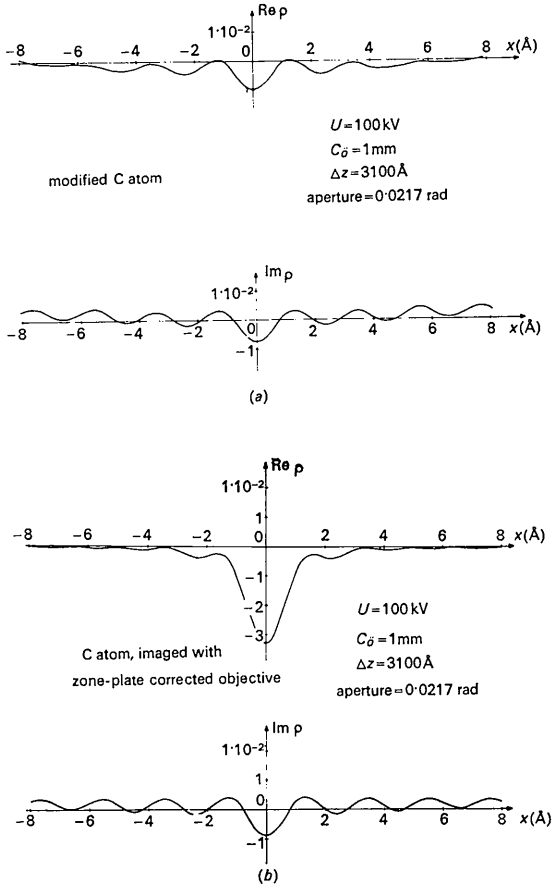

Fig. 6. Strongly defocused C atom image without and with insertion of a zone plate calculated for the pupil function in Fig. 3(*b*). Again, only the real parts will be seen in the bright-field image. Note the low contrast in Fig. 6(*a*), which will make image reconstructions difficult. Additional ripples [not shown in (*a*)] occur at 14, 20 and 23 Å. In Fig. 6(*b*), the resolution is nearly doubled against the corresponding resolution in Fig. 5(*d*). The amplitudes Re ϱ in the image centre are approximately equal in both cases.

Zone-correction plates

Zone-correction plates are inserted into (or near to) the focal plane of the objective. They are filters with transparent regions whose shape depends on the back-modifying function applied. In the ideal case u in equation (8) should be unity and the zone correction plate should be a phase shifting foil formed according to S^- in equation (19).

$$S_0^- = \exp\left[-i(\gamma_0+\pi/2)\right] \quad (19)$$

[see also equation (12)]. A lens equipped with such a correction plate would work like an ideal lens equipped with a Zernike phase-shifting plate. Another back-modifying function is defined in (20):

$$\begin{aligned} S_0^- &= \ \ 1 \text{ for } 0<\gamma_0+\pi/2<\pi\,, \\ S_0^- &= -1 \text{ for } \pi<\gamma_0+\pi/2<2\pi\,. \end{aligned} \quad (20)$$

It leads to a system of concentric annular diaphragms made of a phase-shifting foil (phase shift $=\pi$) of constant thickness. This back-modification will lead to a pupil function according to Fig. 3 with the difference that the negative regions are converted to positive regions by the additional phase shift of π in the phase-shifting foil.

Phase-shifting plates are difficult to apply in electron microscopy as they scatter electrons. This scattering can be avoided if the phase-shifting foil is replaced by annular screens. The back modifying function is defined in (21):

$$\begin{aligned} S_0^- &= 1 \text{ for } 0<\gamma_0+\pi/2<\pi\,, \\ S_0^- &= 0 \text{ for } \pi<\gamma_0+\pi/2<2\pi\,. \end{aligned} \quad (21)$$

In this case the negative regions of the pupil function in Fig. 3 will simply be screened off. Hanszen (1966) proposed to take a set of electron micrographs using a set of zone plates, calibrated for different defocusing parameters. Thus zero regions in the Fourier transform in one micrograph might be supplemented by other micrographs and a combined image could be built up. The experimental difficulties of verifying this scheme might be considerable. It has been shown in detail (Langer & Hoppe, 1966/67, 1967*a*, *b*) that in all of these cases true atomic images will appear at a resolution defined by the diffraction limit. An additional advantage is that the positive region around the image point (Figs. 5 and 6) will disappear. The three back-modifications differ in the noise, (diffraction ripples) which increases from equations (19) to (21). The first experiments with zone-correction plates have already been published (Möllenstedt, Speidel, Hoppe, Langer, Katerbau & Thon, 1968).

It should again be stressed that, according to equation (3), only intensities can be registered. This can lead to difficulties if atoms show considerable

anomalous scattering. If only atoms of one kind are present, then this difficulty can be removed. In this case, the modified structure factor F' (for thin objects) can be written according to equation (22).

$$F'_{x^*y^*} = S_0 \exp i\varphi \sum_{j=1}^{n} |f| \exp 2\pi i(x^*x_j + y^*y_j) . \quad (22)$$

The anomalous phase shift φ can then be introduced into the non-individual modifying function (23).

$$S'_0 = S_0 \exp i\varphi . \quad (23)$$

In the case of objects with different kinds of atoms, a mean anomalous scattering [equation (24)] can be introduced in order to produce, by back-modification, a real and positive amplitude ϱ in approximation.

$$\bar{\varphi} = \sum_{j=1}^{n} \frac{\varphi_j}{n} . \quad (24)$$

With zone-correction plates dark field imaging will be possible because the square of the positive real function ϱ [third term in equation (3)] can be converted into the function itself.

Maréchal-type image reconstruction

As has already been pointed out, the bright-field image (coherent illumination) of a weakly scattering object is in good approximation proportional to the real part $(\varrho+\varrho^*)$ of the image amplitude [equation (3)]. Using equation (24) and neglecting the residual anomalous scattering of the atoms, we obtain the Fourier transform of the registered image for a thin object

$$F'_{x^*y^*} = (S_0 \exp i\bar{\varphi} + S_0^* \exp -i\bar{\varphi}) \sum_{j=1}^{n} |fj| \exp 2\pi i(x^*x_j + y^*y_j) . \quad (25)$$

This Fourier transform may be calculated from the registered image. After correction of F' to the structure factor F of the non distorted structure using the back-modifying function (26)

$$S_0^{-\prime} = (S_0 \exp i\bar{\varphi} + S_0^* \exp -i\bar{\varphi})^{-1} \quad (26)$$

the undistorted image can be calculated.* The Maréchal type modifying function is, in contrast to the modifying functions hitherto discussed, a real function. If there is no anomalous scattering, the modifying function is equal to the imaginary part of the pupil function in Fig. 3. The difficulty is that the back-modifying function (26) will become infinite if the modifying function becomes zero. Weighting functions must, therefore, be used. A simple choice for $S_0^{-\prime}$ is given in (27).

$$\begin{aligned} S_0^{-\prime} &= \ \ 1 \text{ if } S'_0 \text{ is positive} , \\ S_0^{-\prime} &= -1 \text{ if } S'_0 \text{ is negative} . \end{aligned} \quad (27)$$

* As an alternative to calculation, the whole reconstruction process can be made in optical analogue devices.

It can be shown that the image of a zone-correction plate corrected electron microscope according to (20) and a Maréchal-type reconstruction according to (27) will lead to the same result.

It can be seen from equation (25) that the F' will be zero at the nodes of the modifying function regardless of the particular structure studied. Thus, Fourier transformation of an electron micrograph will immediately reveal the constants of the pupil function for this special diagram. These nodes have first been experimentally studied on light diffractograms of electron micrographs of a carbon foil by Thon (footnote *, page 417). These nodes not only reveal spherical aberration and defocusing but also axial astigmatism and drift (Frank, 1970). This objective measure of the constants of the optical path built into every electron micrograph makes it possible to separate unambiguously the structure from aberrations. Hanszen (1968) and Schiske (1968) have proposed to use the Maréchal-reconstruction process for electron microscopy in a special version, in which a series of electron micrographs at different foci will be taken and evaluated. Such an organization of the measurements has the advantage that information lost near the nodes on one diagram can be replaced by information on other diagrams with different defocusing parameters.

Determination of the complex image amplitude

New image reconstruction schemes.

Even the ideal back-modifications (19) and (26) (forgetting the infinity difficulties) are error-free only if the image amplitude ϱ is real. The reason for this is fundamental. The intensity function registered on a photographic plate is real and modifications of that function can only lead to real functions. Only if the image amplitude is real (or can be converted to a real function) can a 1:1 correlation between intensity and amplitude be established. It has already been pointed out that for two reasons [(i) different atoms produce different anomalous scattering, (ii) the structure factors lie on the Ewald sphere] the image amplitude is complex. Using equation (16) to (18) we separate the structure factor F_1 of the 'real' structure from the structure factor F_2 of the 'imaginary' structure.

$$\begin{aligned} F'_{x^*y^*} &= S_0 \sum_{j=1}^{n} (f'_j + if''_j) \exp 2\pi i(x^*x_j + y^*y_j) \\ &= S_0F_1 + iS_0F_2 \\ f'_j + if''_j &= |f_j| \exp i(\varphi_j + 2\pi z^*z_j) \\ F_1 &= \sum_{j=1}^{n} f'_j \exp 2\pi i(x^*x_i + y^*y_j) \\ F_2 &= \sum_{j=1}^{n} f''_j \exp 2\pi i(x^*x_j + yy_j) . \end{aligned} \quad (28)$$

Separating S_0 into real and imaginary parts

$$S_0 = \sigma_0' + i\sigma_0'' \tag{29}$$

we get:

$$F'_{x^*y^*} = \sigma_0' F_1 - \sigma_0'' F_2 - i(\sigma_0'' F_1 + \sigma_0' F_2) = A - iB\,. \tag{30}$$

F', the structure factor which has been modified by the pupil-function, can again be separated into a structure factor of a real structure A and the structure factor of an imaginary structure B. In a coherent bright field, only the structure factor A of the real part of the image amplitude [equation (3)] can be found by Fourier transformation. The important point is that A is a weighted sum of F_1 and F_2. Separation of F_1 and F_2 is possible, if there is a second measurement with other weights σ_0' and σ_0''. Let us assume, for example, that a second exposure is taken under the same conditions the only difference being that a Zernike phase shifting foil (phase shift, $\pi/2$) is inserted into the aperture of the electron microscopic objective. Owing to this additional phase shift, the structure factors B of the imaginary part of the modified image amplitude will now be registered on the plate. These two measurements therefore register the complete complex and modified image amplitude. It can easily be seen from equation (3) that F_1 and F_2 can be calculated from A and B if the coefficients σ_0' and σ_0'' are known. A similar separation of F_1 and F_2 can be achieved if two exposures are taken with a different focus. Then the modification function S_0 will change and thus also the coefficients σ_0' and σ_0'' will have different values. The real and imaginary parts of the structure factors F_1 and F_2 can then be calculated from the measured real and imaginary parts of the structure factors A_1 and A_2 of the two exposures by solving two sets of linear equations with two unknowns.

$$\begin{aligned}
|A_1|\cos\alpha_1 &= \sigma'_{0,1}|F_1|\cos\varphi_1 - \sigma''_{0,1}|F_2|\cos\varphi_2\\
|A_2|\cos\alpha_2 &= \sigma'_{0,2}|F_1|\cos\varphi_1 - \sigma''_{0,2}|F_2|\cos\varphi_2\\
|A_1|\sin\alpha_1 &= \sigma'_{0,1}|F_1|\sin\varphi_1 - \sigma''_{0,1}|F_2|\sin\varphi_2\\
|A_2|\sin\alpha_2 &= \sigma'_{0,2}|F_1|\sin\varphi_1 - \sigma''_{0,2}|F_2|\sin\varphi_2\,.
\end{aligned} \tag{31}$$

The calculation depends on the coefficients σ' and σ'' the Fourier coefficients of which can be calculated with good accuracy from two Maréchal images. Again the lost information can be restored using redundancy principles. Another way is to enlarge the experimental basis taking focusing series; the evalution scheme of Schiske (1968) provides the necessary theoretical basis for such a type of calculations.

Another reconstruction scheme for the determination of the complete complex image amplitude ϱ has recently been proposed by Hoppe, Langer & Thon (1969). The idea is to screen off a semicircle in the aperture plane in order to halve the information which has to be registered on the photographic plate. It is well-known that the Fourier transform of a complex structure has no centre of symmetry. If the other half of the aperture in a second experiment is screened off, the complete information for building up a complex image amplitude from both exposures should be obtained. If one half of the Fourier space is screened off, the amplitude in the image plane ϱ_p is given by the partial Fourier transform (32).

$$\varrho_{1,p} = C\int_0^\infty\int_{-\infty}^\infty F'_{x^*y}\exp\left[-2\pi i(x^*x+y^*y)\right]\mathrm{d}x^*\mathrm{d}y^*\,. \tag{32}$$

The image amplitude, generated by the scattered rays through the other semicircle has the form

$$\varrho_{2,p} = C\int_0^\infty\int_{-\infty}^\infty F'_{x^*-y^*}\exp\left[-2\pi i(x^*x+y^*y)\mathrm{d}x^*\mathrm{d}y^*\,. \tag{33}$$

$\varrho_{1,p}$ and $\varrho_{2,p}$ are complex, corresponding to the extreme asymmetry in reciprocal space. Now the photographic plate only registers $(\varrho+\varrho^*)$. $\varrho^*_{1,p}$ is simply the conjugate complex function of $\varrho_{1,p}$, given in equation (34).

$$\varrho^*_{1,p} = C\int_0^\infty\int_{-\infty}^\infty F'^*_{x^*y^*}\exp 2\pi i(x^*x+y^*y)\mathrm{d}x^*\mathrm{d}y^*\,. \tag{34}$$

The second term in equation (3) can, therefore, be written after some trigonometric transformations (35),

$$\begin{aligned}
I_0(\varrho_{1,p}+\varrho^*_{1,p}) = 2I_0C\int_0^\infty\int_{-\infty}^\infty |F_{x^*y^*}|\cos\Omega\cos 2\pi(x^*x\\
+y^*y)\mathrm{d}x^*\mathrm{d}y^* + 2I_0C\int_0^\infty\int_{-\infty}^\infty |F_{x^*y^*}|\\
\times\sin\Omega\sin 2\pi(x^*x+y^*y)\mathrm{d}x^*\mathrm{d}y
\end{aligned} \tag{35}$$

where

$$\Omega = \varphi_{x^*y^*} + \gamma_0 + \pi/2\,. \tag{36}$$

It can immediately be seen that equations (35) and (36) give the theoretical basis for an excellent image reconstruction process. A Fourier analysis of the intensity function on the photographic plate delivers the absolute values $|F_{x^*y^*}|$ of the correct structure and the phases Ω without a weighting function which lowers the accuracy, in contrast with the Maréchal reconstruction. The phases Ω are incorrect but using expression (36) they can most easily be converted into the correct phases $\varphi_{x^*y^*}$. It is obvious that the same reconstruction can be made with $\varrho_{2,p}$. In the same paper, a reconstruction process has also been described, which needs only one exposure for the determination of the Fourier coefficients of the complex structure. This is at first surprising as it seems to violate our postulate that the double information of a complex structure cannot be registered in a real structure. The answer is that the image of the photographic plate has in one direction twice the resolution required for the electron microscopic image. Therefore, twice the information can be stored on the photographic plate. This reconstruction scheme will not be discussed in this paper, as it cannot be done with data taken in a conventional

electron microscope. Instead of bright field imaging, where the primary wave is the reference wave, a special illuminating system must be used which delivers a separate reference wave (as in holography) which is inclined against the primary wave. A third image correction process for complex functions using inclined illumination (described in the same paper and not reported here) can only be used for very thin specimens.

In the case of a focused ideal lens γ_0 in equation (36) becomes zero. In the case of a phase object, the image will resemble the first derivative of the Fourier transform. The atoms will consist of two equal parts, one with positive and the other with negative contrast.

The determination of the complex image amplitude has an additional implication in electron structure analysis. The anomalous phase shift φ for heavy atoms is appreciably greater than for light atoms. If one calculates the real and the imaginary parts of the structure, the relation between the weights of light and heavy atoms is different. It will therefore be possible to calculate a weighted difference image which will show only one kind of atom. Thus, a physical image difference method, with implications similar to the chemical image difference method (Hoppe, Langer Frank & Feltynowski, 1969), can be established. It has already been pointed out that the half screen reconstruction process delivers amplitudes and phases for all Fourier coefficients with the same accuracy. It is therefore advisable to use it also in cases where ϱ is real. Then only one exposure is necessary. A third exposure (or in the case of a real ϱ, and second exposure) of the Maréchal type might be useful for the determination of the optical constants.*

Difficulties with reconstruction schemes

The zone correction scheme has the advantage that the images of the atoms peak up in the electron diagram to small regions with high contrast. This is no longer the case if one uses reconstruction schemes. The atoms are spread over wide regions in real space and the image of a single atom has, therefore, low contrast. If the object is much larger than the atom, then the contrast difficulties might partly disappear, as the contrast is enhanced by the overlapping of the atomic images. In any case it is advantageous to choose the optical parameters, especially the defocusing term, in such a way that the size of the distorted atoms is also as small as possible. Especially in the case of very small objects or of objects which have the structure of a narrow fibre, this point might be important. Another difficulty will appear if only a small region of an electron micrograph is studied. Other regions of the micrograph may no longer simply be screened off. It can be seen that at the border of this region atoms will be mutilated whereas parts of atoms outside this region will contribute to the structure within that region. Again, only if the studied region in an electron micrograph is much larger than the size of the atom can these border difficulties be neglected. This effect can be demonstrated if one takes light diagrams of large and small regions of an electron micrograph. The multilated atoms do not have the same Fourier transform as the unmutilated ones and they add a background which obscures the nodes. Figs. 7 and 8 show examples. If the physical size of the object is limited, then half of the virtual size of the distorted atoms has to be added at the borders (Fig. 9) to the region taken for reconstruction, if an error-free reconstruction is to result. The demand for a limited object in space is difficult to accomplish as every molecular object has to be supported in some way. Perhaps the combination of the image difference methods with reconstruction methods might be the answer.

These difficulties make it improbable that image reconstruction methods will entirely replace zone correction methods. There is another argument in favour of this conclusion. Electron diagrams taken with zone correction methods deliver a good approximation of the structure without calculation. It is quite probable that real structure research will be done on small particles, on small regions and in three dimensions. But it will be impossible to do such research if it cannot be preceded by a search of electron micrograms in a conventional way. It is beyond question that micrographs at high resolution with atomic peaks corrected for aberrations of different kind provide the best basis for such a search. Reconstruction methods will be necessary in order to check whether there are any errors in focus, axial astigmatism *etc.*

The use of redundancies in electron structure research

As has already been pointed out, the most successful use of redundancies occurs in X-ray crystal structure analysis. In many cases, the knowledge of the basic structural features of an atomic structure makes it possible to recover the phase information knowing only the absolute values of the Fourier coefficients. This type of information loss does not occur in electron structure research using the methods discussed in this paper, but with some methods, further information loss can lead to difficulties. Let us assume that a zone correction plate has been used which screens off structure factors with wrong (opposite) phases. It has already been pointed out that real atomic images are formed, despite the lack of approximately half the information, but the background noise might obscure atoms in unfortunate cases. If the amplitudes and phases of the lost structure factors could be restored by calculation, then an ideal structure image could be synthesized.

* Structural changes induced by radiation are, therefore, unimportant for these measurements.

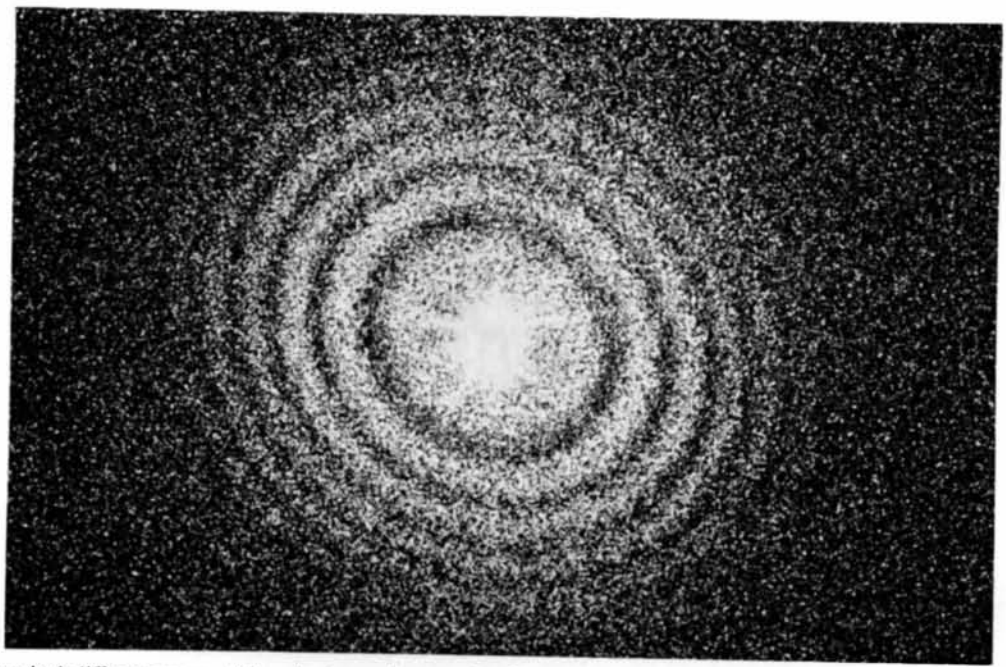

Fig. 7. Light-optical diffractogram of the electron micrograph of an amorphous carbon foil (Thon, 1966), with bright field, strongly underfocused image, $U=100$ kV. The diffractogram corresponds to an object region of 1000 Å Ø (circular aperture in the diffractometer 2 cm Ø); due to the large object region, the nodes in the imaginary part of the pupil function appear very clearly in the diffractogram.

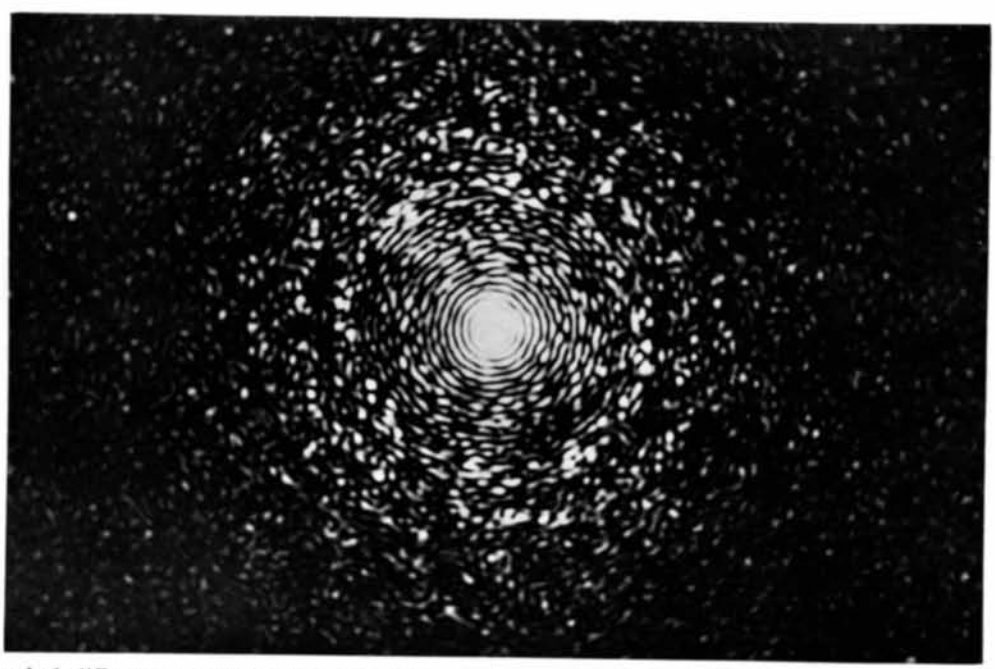

Fig. 8. Light-optical diffractogram (from the same electron micrograph as in Fig. 7) from an object region which is so small (200 Å Ø; aperture in the diffractometer 0·4 cm Ø) that the nodes, visible in Fig. 7, are already obscured.

To face p. 424

Ways for the introduction of redundancy principles are discussed below.

1. *Squaring* (Sayre, 1952) *and phase correction* (Hoppe & Gassmann, 1968).

These procedures are based on the fact that (three-dimensional) atomic structures consist of resolved positive peaks. In X-ray crystallography, they can be used to determine or to correct phases. It is easy to show that both procedures yield amplitudes and phases of structure factors which have not been measured. The calculation of the missing structure factors has to be done in an iterative process. The newly determined structure factors will be added in the next cycle to the whole set of structure factors which then forms the basis for the next calculation of structure factors. Convergence is achieved when a calculation of the measured structure factors yields the measured values themselves.

This scheme needs resolved atoms and can, therefore,only be applied if three-dimensional methods are used. In order to check the idea, we have made the following test calculations. We divided the reciprocal space of different crystal structures into equidistant spherical zones with a thickness of the dimension of the unit cell. We then calculated the crystal structures, setting the structure factors in the even (or odd) zones to zero. In all cases, we again found the atomic structure which was partly obscured by a high background noise. The important point is that phase correction starting from these incomplete sets revealed the complete set with high accuracy.*

2. *Redundancy due to an object of finite size*

Procedures based on this redundancy principle have no counterpart in X-ray crystallography. They are based on the sampling theorem of Whittaker (1915) and Shannon (1949). The advantage is that atomic resolution is not necessary. Therefore, this restoration of Fourier coefficients can also be done in two dimensions or at less than atomic resolution.

We assume that the object is limited by a rectangle with the edges a and b. Then the Fourier coefficients of the continuous Fourier transform can be replaced by the discontinuous Fourier coefficients (structure factors) F_{hk} of the reciprocal lattice with the unit-cell dimensions a^* and b^*. The corresponding Fourier synthesis yields a lattice with the unit-cell dimensions a and b in which every cell contains the object information. The Whittaker–Shannon theorem simply states that the aperiodic object, and thus the continuous Fourier transform, can be restored if the lattice is multiplied with a rectangle function which is 1 inside and 0 outside the rectangle a,b. The corresponding convolution in reciprocal space can be written

$$F_{x_j^* y_j^*} = \sum_h \sum_k F_{hk} C_{hkj} , \qquad (37)$$

where

$$C_{hkj} = \frac{\sin \pi(ax_j^* - h) \sin \pi(by_j^* - k)}{\pi(ax_j^* - h)\pi(by_j^* - k)} .$$

Equation (37) can be used in two ways. Knowing $F_{h,k}$, every value $F_{x_j^* y_j^*}$ of the continuous Fourier transform can be calculated. On the other hand, if at least as many $F_{x_j^* y_j^*}$ have been measured as there are $F_{h,k}$ to be determined, then the $F_{h,k}$ can be solved assuming that equation (37) constitutes a set of linear equations with $F_{h,k}$ unknowns. The important point is that owing to the redundancy resulting from the finite size of the object, even a partial measurement of the Fourier transform contains enough information to construct the image.

It should be mentioned that this restoration scheme was first proposed to increase the resolution limit in microscopy (Barnes, 1966) and for three-dimensional reconstruction of images in electron microscopy (Hoppe, 1969). In the latter case, it is evident that the three-dimensional reconstruction can start immediately from the three-dimensional generalization of equation (37) using a partial knowledge of the continuous Fourier transforms of a number of projections of the tilted object. It stands to reason that both redundancy principles can be used in a combined way.

* Details of these calculations will be published elsewhere.

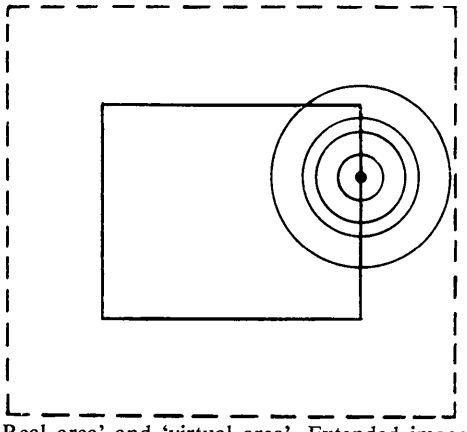

Fig. 9. 'Real area' and 'virtual area'. Extended image points need for correct Fourier transformation the larger area with the dotted border. If the image points are pointlike, the smaller area will be sufficient (*cf.* Figs. 7 and 8).

This work has been supported by the Deutsche Forschungsgemeinschaft, the Fonds der Chemischen Industrie and the Badische Anilin- & Soda-Fabrik. We should like to express our sincere thanks.

References

BARNES, C. W. (1966). *J. Opt. Soc. Amer.* **56**, 575.
FRANK, J. (1970). *Optik.* **20**, 171.
GLASER, W. (1952). *Grundlagen der Elektronenoptik.* Berlin: Springer.
HANSZEN, K. J. (1966). *Fachber. Physikertg. München*, 94.
HANSZEN, K. J. (1968). 4. *Europ. Reg. Conf. Electron Microscopy, Rome.* Vol. I, p. 153.

HOPPE, W. (1961). *Naturwissenschaften*, **48**, 736.
HOPPE, W. (1963). *Optik*, **20**, 599.
HOPPE, W. (1969). *Optik*. **29**, 617.
HOPPE, W. & GASSMANN, J. (1968). *Acta Cryst.* B**24**, 97.
HOPPE, W., LANGER, R., FRANK, J. & FELTYNOWSKI, A. (1969). *Naturwissenschaften*, **56**, 267.
HOPPE, W., LANGER, R., KNESCH, G. & POPPE, CH. (1968). *Naturwissenschaften*, **55**, 333.
HOPPE, W., LANGER, R. & THON, F. (1970). *Optik*, **30**, 538.
KLUG, A. & BERGER, J. E. (1964). *J. Mol. Biol.* **10**, 565.
LANGER, R. & HOPPE, W. (1966/67). *Optik*, **24**, 470.
LANGER, R. & HOPPE, W. (1967*a*). *Optik*, **25**, 413.
LANGER, R. & HOPPE, W. (1967*b*). *Optik*, **25**, 507.
MARÉCHAL, A. & CROCE, P. (1953). *C. R. Acad. Sci. Paris*, **237**, 607. See also TSUJIUCHI, J. (1963) in *Progress in Optics*, Vol. II, 133 ff. Amsterdam: North Holland Publ. Co.; and for theoretical treatment, ELIAS, P., GREY D. S. & ROBINSON, D. Z. (1952). *J. Opt. Soc. Amer.* **42**, 127.
MÖLLENSTEDT, G., SPEIDEL, R., HOPPE, W., LANGER, R., KATERBAU, K.-H. & THON, F. (1968). 4. *Europ. Reg. Conf. Electron Microscopy, Rome*, 1968. Vol. I, p.25. 1
DEROSIER, D. J. & KLUG, A. (1968). *Nature, Lond.* **217**, 130.
RUSKA, E. (1965). *Optik*, **22**, 319.
SAYRE, D. (1952). *Acta Cryst.* **5**, 60.
SCHERZER, O. (1949). *J. Appl. Phys.* **20**, 20.
SCHERZER, O. & TYPKE, D. (1967/68). *Optik*, **26**, 564.
SCHISKE, P. (1968). 4. *Europ. Reg. Conf. Electron Microscopy, Rome* 1968. Vol. I, p. 145.
SHANNON, C. E. (1949). *Proc. IRE*, **37**, 10.
THON, F. (1966). *Z. Naturforschung*, **21***a*, 476.
WASER, J. & SCHOMAKER, V. (1953). *Rev. Mod. Phys.* **25**, 671.
WHITTAKER, E. T. (1915). *Proc. Roy. Soc. Edinburgh*, A**35**, 181.
ZERNIKE, F. (1935). *Phys. Z.* **36**, 848.

Acta Cryst. (1970). A**26**, 426

Arcing Phenomenon in Single Crystals of Cadmium Bromide

BY V. K. AGRAWAL* AND G. C. TRIGUNAYAT
Department of Physics and Astrophysics, University of Delhi, Delhi-7, India

(*Received* 8 *September* 1969)

Solution-grown single crystals of cadmium bromide have been found to exhibit arcing phenomena on their oscillation photographs and to give rise to closed rings of various shapes and sizes on Laue photographs. These have been explained in terms of the formation, during crystal growth, of tilt boundaries consisting of edge dislocations created by simultaneous slip along more than one close-packed direction on different basal and non-basal planes. The measurement of arc lengths on these oscillation photographs enables an estimate of the density of dislocations within the boundaries to be made.

Introduction

This X-ray study of single crystals of cadmium bromide is one in a series of studies on phenomena of arcing and polytypism in the MX_2 compounds, which have close-packed hexagonal layer structures. Other substances of this type, *viz.* CdI_2 and PbI_2, have already been investigated (Agrawal & Trigunayat, 1969*a*,*b*; Agrawal, Chadha & Trigunayat, 1970). Practically all the 12 crystals investigated in this study exhibit arcing phenomena on their X-ray photographs. This contrasts strongly with only 5% such instances in PbI_2 crystals and 42% in CdI_2 crystals. Reflexions of various shapes, *viz.* sigma, triangular ring, hexagonal ring, double rings, *etc.*, have been observed on the Laue photographs. They have been explained in terms of tilt boundaries formed by vertical alignment of edge dislocations created by slip along more than one closest-packed direction on different basal and non-basal planes. In the crystals of CdI_2 and PbI_2 investigated earlier, the slip was found to be confined to the basal planes alone.

Experimental methods

The crystals were grown from aqueous solutions. At room temperature, 5 g of reagent grade $CdBr_2.4H_2O$ were dissolved in 20 cc of ordinary tap water in a shallow crystallizing dish. Hydrobromic acid was also added to prevent the formation of the hydrated bromide which forms in purely aqueous solutions. After several days, hexagonal crystal platelets of cadmium bromide, up to 1 mm across and 0.1 mm thick, formed in the dish. They were carefully removed from the solution and tested for perfection in a polarizing microscope before being mounted on the X-ray camera in order to obtain oscillation and Laue photographs. The *a* axis oscillation photographs were taken in the range 19 to 34°, *i.e.* the angle (referred to as φ in the following) between the incident X-ray beam and the *c* axis varied between 19 and 34°. This range was

* Present address: Department of Physics, Hastinapur College, Moti Bagh, New Delhi-23, India.